

Measuring temporally complex ultrashort pulses using multiple-delay crossed-beam spectral interferometry

Jacob Cohen*, Pamela Bowlan, Vikrant Chauhan, and Rick Trebino

Georgia Institute of Technology, School of Physics 837 State St, Atlanta, GA 30332 USA

*jcohen7@gatech.edu

Abstract: We introduce a spectral-interferometry (SI) technique for measuring the complete intensity and phase of relatively long and very complex ultrashort pulses. Ordinarily, such a method would require a high-resolution spectrometer, but our method overcomes this need. It involves making multiple measurements using SI (in its SEA TADPOLE variation) at numerous delays, measuring many temporal pulselets within the pulse, and concatenating the resulting pulselets. Its spectral resolution is the inverse delay range—many times higher than that of the spectrometer used. Our simple proof-of-principle implementation of it provided 71 fs temporal resolution and a temporal range of 100 ps using a few-cm low-resolution spectrometer.

©2010 Optical Society of America

OCIS codes: (320.0320) Ultrafast optics; (320.7100) Ultrafast measurements

References and Links

1. D. J. Geisler, N. K. Fontaine, R. P. Scott, J. P. Heritage, K. Okamoto, and S. Yoo, "360-Gb/s optical transmitter with arbitrary modulation format and dispersion precompensation," *IEEE Photon. Technol. Lett.* **21**(7), 489–491 (2009).
2. H. Valtna-Lukner, P. Bowlan, M. Löhmus, P. Piksarv, R. Trebino, and P. Saari, "Direct spatiotemporal measurements of accelerating ultrashort Bessel-type light bullets," *Opt. Express* **17**(17), 14948–14955 (2009).
3. Z. Jiang, C.-B. Huang, D. E. Leaird, and A. M. Weiner, "Optical arbitrary waveform processing of more than 100 spectral comb lines," *Nat. Photonics* **1**(8), 463–467 (2007).
4. W. S. Warren, H. Rabitz, and M. Dahleh, "Coherent control of quantum dynamics: the dream is alive," *Science* **259**(5101), 1581–1589 (1993).
5. R. Trebino, *Frequency-Resolved Optical Gating: The Measurement of Ultrashort Laser Pulses* (Kluwer Academic Publishers, Boston, 2002).
6. C. Froehly, A. Lacourt, and J. C. Vienot, "Time impulse response and time frequency response of optical pupils: Experimental confirmations and applications," *Nouvelle Revue D'Optique* **4**(4), 183–196 (1973).
7. P. Bowlan, P. Gabolde, A. Shreenath, K. McGresham, R. Trebino, and S. Akturk, "Crossed-beam spectral interferometry: a simple, high-spectral-resolution method for completely characterizing complex ultrashort pulses in real time," *Opt. Express* **14**(24), 11892–11900 (2006).
8. A. P. Kovács, K. Osvay, Z. Bor, and R. Szipöcs, "Group-delay measurement on laser mirrors by spectrally resolved white-light interferometry," *Opt. Lett.* **20**(7), 788–790 (1995).
9. J. P. Geindre, P. Audebert, S. Rebibo, and J. C. Gauthier, "Single-shot spectral interferometry with chirped pulses," *Opt. Lett.* **26**(20), 1612–1614 (2001).
10. D. Meshulach, D. Yelin, and Y. Silberberg, "Real-time spatial-spectral interference measurements of ultrashort optical pulses," *J. Opt. Soc. Am. B* **14**(8), 2095–2098 (1997).
11. K. Misawa, and T. Kobayashi, "Femtosecond Sagnac interferometer for phase spectroscopy," *Opt. Lett.* **20**(14), 1550–1552 (1995).
12. P. Bowlan, P. Gabolde, M. A. Coughlan, R. Trebino, and R. J. Levis, "Measuring the spatiotemporal electric field of ultrashort pulses with high spatial and spectral resolution," *J. Opt. Soc. Am. B* **25**(6), A81–A92 (2008).
13. L. Lepetit, G. Chériaux, and M. Joffre, "Linear techniques of phase measurement by femtosecond spectral interferometry for applications in spectroscopy," *J. Opt. Soc. Am. B* **12**(12), 2467–2474 (1995).
14. P. Bowlan, P. Gabolde, and R. Trebino, "Directly measuring the spatio-temporal electric field of focusing ultrashort pulses," *Opt. Express* **15**(16), 10219–10230 (2007).
15. P. Bowlan, H. Valtna-Lukner, M. Löhmus, P. Piksarv, P. Saari, and R. Trebino, "Measuring the spatiotemporal field of ultrashort Bessel-X pulses," *Opt. Lett.* **34**(15), 2276–2278 (2009).

16. P. Bowlan, U. Fuchs, R. Trebino, and U. D. Zeitner, "Measuring the spatiotemporal electric field of tightly focused ultrashort pulses with sub-micron spatial resolution," *Opt. Express* **16**(18), 13663–13675 (2008).
17. M. A. Foster, R. Salem, D. F. Geraghty, A. C. Turner-Foster, M. Lipson, and A. L. Gaeta, "Silicon-chip-based ultrafast optical oscilloscope," *Nature* **456**(7218), 81–84 (2008).
18. J. E. Heebner, and C. H. Sarantos, "Progress towards the solid-state all-optical streak camera," in *Conference on Lasers and Electro-Optics (CLEO)*, (Optical Society of America, 2009), CThW1.
19. V. R. Supradeepa, D. E. Leaird, and A. M. Weiner, "Single shot amplitude and phase characterization of optical arbitrary waveforms," *Opt. Express* **17**(16), 14434–14443 (2009).
20. N. K. Fontaine, R. P. Scott, J. P. Heritage, and S. J. B. Yoo, "Near quantum-limited, single-shot coherent arbitrary optical waveform measurements," *Opt. Express* **17**(15), 12332–12344 (2009).
21. H. Miao, D. E. Leaird, C. Langrock, M. M. Fejer, and A. M. Weiner, "Optical arbitrary waveform characterization via dual-quadrature spectral shearing interferometry," *Opt. Express* **17**(5), 3381–3389 (2009).
22. B. Rubin, and R. M. Herman, "Monochromators as light stretchers," *Am. J. Phys.* **49**(9), 868 (1981).
23. N. H. Schiller, and R. R. Alfano, "Picosecond characteristics of a spectrograph measured by a streak camera/video readout system," *Opt. Commun.* **35**(3), 451–454 (1980).
24. C. Dorrer, N. Belabas, J.-P. Likhforman, and M. Joffe, "Spectral resolution and sampling issues in Fourier-transform spectral interferometry," *J. Opt. Soc. Am. B* **17**(10), 1795–1802 (2000).
25. P. O'Shea, M. Kimmel, X. Gu, and R. Trebino, "Highly simplified device for ultrashort-pulse measurement," *Opt. Lett.* **26**(12), 932–934 (2001).
26. V. Chauhan, P. Bowlan, J. Cohen, and R. Trebino, "Single-diffraction-grating and grism pulse compressors," *J. Opt. Soc. Am. B* **27**(4), 619–624 (2010).
27. A. S. Welington, and D. H. Auston, "Novel sources and detectors for coherent tunable narrow-band terahertz radiation in free space," *J. Opt. Soc. Am. B* **13**(12), 2783–2791 (1996).
28. C. Dorrer, and I. Kang, "Linear self-referencing techniques for short-optical-pulse characterization," *J. Opt. Soc. Am. B* **25**(6), A1–A12 (2008).
29. R. R. Alfano, and S. L. Shapiro, "Observation of self-phase modulation and small-scale filaments in crystals and glasses," *Phys. Rev. Lett.* **24**(11), 592–594 (1970).

1. Complex ultrafast waveforms and their measurement

Currently, there is great interest in the generation of arbitrary complex ultrafast waveforms in time, typically ~ 1 ns long with ~ 100 fs substructure, for telecommunications [1], frequency combs [2,3], coherent control, and spectroscopy [4]. However, measurement techniques to precisely measure both the intensity and phase of such pulses do not yet exist.

Femtosecond pulses are very well characterized using a variety of methods, including frequency-resolved optical gating (FROG) [5] and spectral interferometry (SI) [6]. Counter-intuitively, the development of techniques for measuring longer pulses from many ps to 1 ns (even simple ones) has lagged far behind those for measuring shorter fs pulses. This is because many-ps pulses are still too short to be well resolved in time, and, from the classical uncertainty principle, such relatively long pulses can have narrow spectral features, which also can be difficult to resolve. A pulse with a temporal length of Δt exhibits spectral features $\delta\omega \sim 1/\Delta t$ wide, which must be resolved for its measurement. The complete measurement of fs near-IR pulses requires an easily attained spectral resolution of only ~ 1 nm. But any frequency- or time-frequency-domain measurement of, say, a 100 ps, 800 nm pulse requires a difficult-to-attain spectral resolution of < 0.01 nm. If the pulse also has 100 fs temporal structure, then, by a similar uncertainty-principle argument, it simultaneously requires a spectral *range* of > 10 nm—a difficult combination of capabilities. The spectral-resolution problem is exacerbated in standard Fourier-transform SI (FTSI) by its requirement of an additional factor of ~ 5 in spectral resolution in order to reconstruct the unknown pulse from the interferogram.

In its favor, SI is conceptually very simple: it involves simply measuring the spectrum of the sum of a known reference pulse and the unknown pulse. The pulses are aligned to have a separation in time of about five pulse lengths (to yield spectral fringes, which yield a simple pulse-retrieval procedure), hence the additional factor-of-five required spectral resolution. Despite its theoretical simplicity, SI is, in practice, very difficult to perform. In addition to the higher spectral resolution it requires, it is also hampered by numerous spatial alignment issues associated with its requirement of perfectly collinear beams. As a result, over the past few years, we have developed an experimentally simpler version of it, called SEA TADPOLE [7].

It involves overlapping the unknown and reference pulses in time and crossing the beams in space in a direction perpendicular to the frequency axis at the spectrometer's camera. Its use of crossed beams rather than collinear beams and its use of fibers to introduce the beams into the device significantly ease the burden of alignment associated with standard SI. Additionally, its use of temporally overlapped pulses allows the pulse's frequency-domain field, $E(\omega)$, to be retrieved without loss of spectral resolution [8–11], and SEA TADPOLE often achieves spectral super-resolution, because it measures the pulse's complex spectral electric field, rather than the simple spectrum. The result is that it can measure very complicated, relatively long pulses easily.

Using SEA TADPOLE, we have been able to measure pulses with time-bandwidth products as large as ~ 400 [7,12], using only a simple few-cm spectrometer—a measurement that would require a $\sim 1/2$ m spectrometer using standard SI. SEA TADPOLE is a significant improvement over standard SI for measuring the temporal electric field of complex pulses.

There are several variations on this idea that also avoid the spectral-resolution loss associated with FTSI [13]. What distinguishes SEA TADPOLE is its use of optical fibers as the pulse input conduit, so it also has spatial resolution and so can be used to measure the pulse in time and space by scanning the entrance fiber across the beam. We have used this approach to measure the spatiotemporal field of focusing pulses [12,14] and Bessel-X pulses [2,15]. Furthermore, we have used near-field scanning optical microscopy probes to simultaneously achieve sub-micron spatial resolution and high spectral resolution [16].

Here we extend the temporal range of SEA TADPOLE to measure the complete temporal intensity and phase of even longer and more complex arbitrary waveforms. Rather than using a reference pulse at just one delay, as in standard SI and SEA TADPOLE, we use *many delays*, making SEA TADPOLE traces for all temporal slices of the long pulse and then concatenate them to reconstruct the entire pulse in time. We call this technique Multiple Delay for Temporal Analysis by Dispersing a Pair of Light E-fields (MUD TADPOLE). The effective spectral resolution of MUD TADPOLE is many times that of SEA TADPOLE, and it is independent of the spectral resolution of the spectrometer. Instead, the spectral resolution is equal to the reciprocal of the reference-pulse delay range. In other words, it can measure pulses as long as the delay that can be generated. Since it is much easier to generate delay than to improve spectral resolution, this is a significant advantage, akin to that of Fourier-transform spectrometers over grating spectrometers, but without the stringent alignment issues.

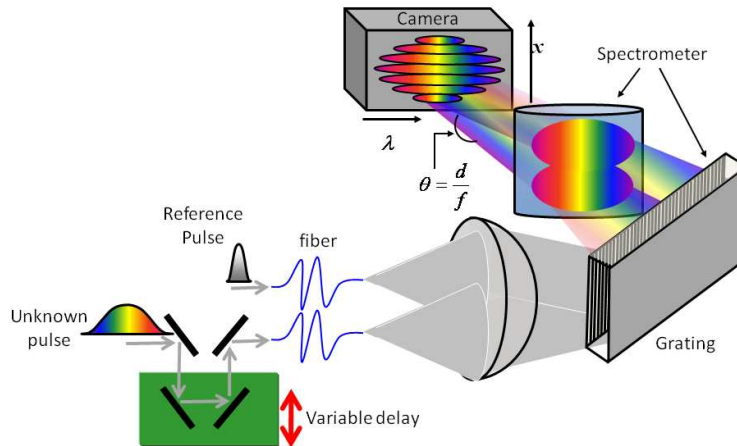


Fig. 1. Experimental setup for MUD TADPOLE. Both the unknown pulse and the reference pulse are coupled into two equal-length single-mode fibers. The unknown pulse passes through a delay stage, which provides the variable delay. Although here it is shown that the unknown pulse is delayed with respect to the reference, it is inconsequential which pulse is delayed with respect to the other. In the horizontal dimension, the light is collimated by the spherical lens and spectrally resolved by the spectrometer. In the vertical dimension, the beams cross at a slight angle resulting in spatial fringes at the camera.

Other techniques for measuring arbitrary waveforms have been proposed. Several time-domain techniques have been introduced [17,18]. One such method has measured pulses up to 100 ps long with 220 fs resolution yielding a record length-to-resolution ratio of 455 [17]. Unfortunately, these methods measure only the intensity, and not the phase.

Several variations on spectral interferometry have been introduced. One variation of SI, known as dual-quadrature SI (DQSI), which does not suffer from the spectral-resolution reduction issue of FTSI [13], was recently reported by Weiner and coworkers and is capable of measuring pulses up to 100 ps in length with 1 ps resolution, resulting in a temporal range-to-temporal resolution ratio of 100 [19]. The measurement of 200 ps-long pulses has also been reported using four-quadrature spectral interferometry, another variation of SI [20]. Furthermore, Weiner and coworkers demonstrated a modified version of DQSI using spectral shearing and a periodically poled LiNbO₃ (PPLN) waveguide called dual quadrature spectral shearing interferometry to measure complex frequency combs up to 30 ps in length [21]. However, all of these variations of SI retain the alignment issues of standard SI.

In contrast, MUD TADPOLE is easily aligned and places no constraints on the pulse being measured (except for SI's usual condition that the reference pulse spectrum contain that of the unknown pulse). Using a simple Fourier-filtering algorithm, MUD TADPOLE directly retrieves both the intensity and phase of the unknown pulse. Additionally, it can in principle be easily extended to measure extremely complex nanosecond long pulses with fs resolution, achieving temporal range-to-temporal resolution ratios of $\sim 210,000$, while measuring complex pulses with time-band-width products of $\sim 70,000$.

Although the version of MUD TADPOLE that we discuss here is a multi-shot technique, we believe that the long temporal range, or equivalently its high spectral resolution, provides a substantial improvement to the field of arbitrary waveform metrology. Furthermore, we are working on a single-shot version and will report on it in a future publication.

2. MUD TADPOLE: Extending SEA TADPOLE to longer pulses

The condition that the length of a pulse measured by SEA TADPOLE is limited to the inverse spectral resolution of the spectrometer can also be expressed in terms of the temporal length of the reference pulse at the *output* of the spectrometer. A fundamental, but often overlooked,

property of spectrometers is that they stretch ultrashort pulses [22]. This has been experimentally verified for ps pulses [23] and fs pulses [12] by measuring the pulse at the output of a spectrometer.

This is easily understood by considering that spectrometers map a small range of frequencies, $\delta\omega$, equal to the spectral resolution, to each pixel of the detector. From the uncertainty principle, such a narrow band of frequencies can only be contained in a pulse that has a temporal duration:

$$\tau_{sp} \geq \frac{1}{\delta\omega}. \quad (1)$$

Therefore, the reference pulse broadens in time inside the spectrometer by the reciprocal of the spectrometer's spectral resolution, τ_{sp} . Because SEA TADPOLE (and other SI techniques) requires the formation of fringes, it also requires temporal overlap of the reference and unknown pulses. Thus it can, at best, be used to measure a pulse only τ_{sp} long. (In principle, the same broadening occurs to the unknown pulse, but the unknown pulses of interest here are, by assumption, already as long as, or longer than, τ_{sp} , so their temporal duration is assumed to be negligibly broadened by the spectrometer.)

In order to measure longer pulses, SEA TADPOLE must be outfitted with a higher resolution spectrometer, which would yield a longer τ_{sp} . Unfortunately, high-resolution spectrometers are extremely large, inconvenient, and expensive due to the proportional relationship between a spectrometer's spectral resolution and number of grooves illuminated on the grating (and hence its size).

Instead of using a high-resolution spectrometer, we introduce a technique that uses a delay stage to scan the unknown pulse in time, resulting in multiple SEA TADPOLE measurements at different delays. Each SEA TADPOLE measurement retrieves a different temporal section of the electric field of the unknown pulse, where the range of each individual measurement is τ_{sp} , and is much shorter than the unknown pulse duration. The retrieved spectral fields are then Fourier transformed to the time domain yielding the retrieved section of the unknown pulse in time. Lastly, the retrieved sections are concatenated in time to reconstruct the entire unknown pulse.

3. MUD TADPOLE retrieval algorithm

The MUD TADPOLE retrieval algorithm consists of three parts, a spatial Fourier-filtering step, a temporal filtering step, and concatenation.

MUD TADPOLE Retrieval Algorithm

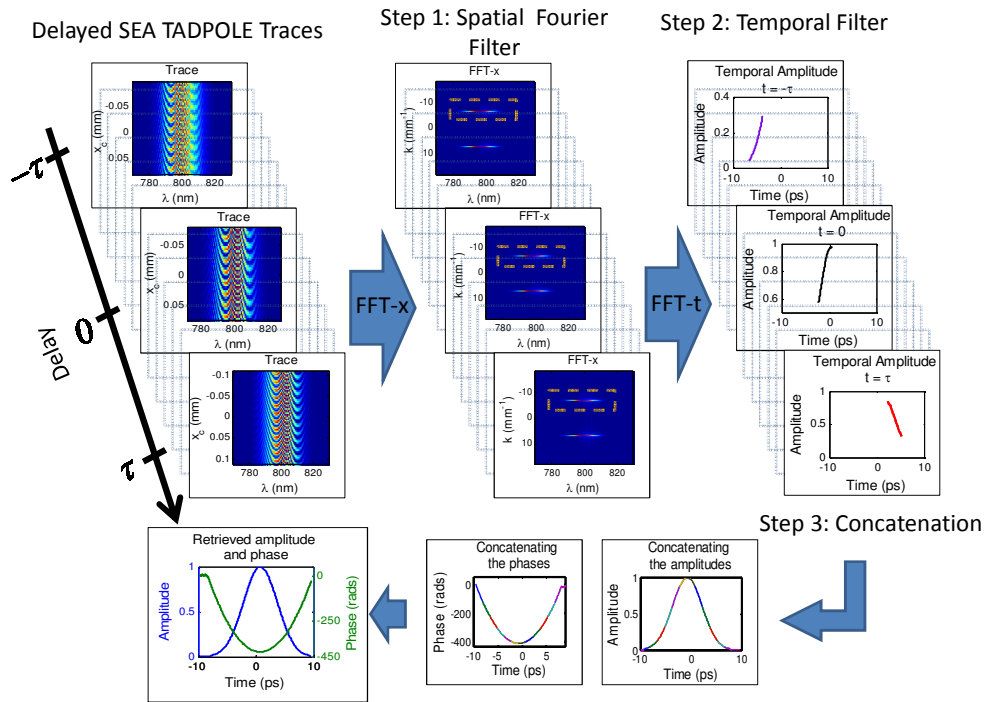


Fig. 2. The MUD TADPOLE retrieval algorithm using simulated data. In Step 1, each SEA TADPOLE trace—corresponding to a different temporal slice—is spatially Fourier filtered, resulting in the electric field at each delay, $E_i(\omega)$. In Step 2, the retrieved fields are temporally filtered, keeping only the region in which the unknown and reference pulses are temporally overlapped. Each retrieved field, $E_i(\omega)$, is Fourier transformed to the time domain and temporally shifted to the lab frame yielding $\tilde{E}_{i,lab}(t - \tau_i)$. In the figure, each color represents the retrieved field at a different delay. Although, only the amplitudes are shown, after re-phasing, the same process is done with the retrieved phases. In Step 3, the retrieved amplitude and phase are separately concatenated using a weighted average, resulting in the retrieval of the entire unknown pulse.

3.1 Spatial Fourier filtering

The first step of the MUD TADPOLE pulse-retrieval algorithm is identical to the SEA TADPOLE Fourier-filtering algorithm [7,9]. In SEA TADPOLE, the electric field of the unknown pulse is retrieved from a spectrally resolved spatial interferogram resulting from the crossing of two beams. The interferogram is given by the following equation:

$$S(x_c, \omega) = S_{ref}(\omega) + S_{unk}(\omega) + 2\sqrt{S_{ref}(\omega)}\sqrt{S_{unk}(\omega)}\cos(2kx_c \sin \theta + \varphi_{unk}(\omega) - \varphi_{ref}(\omega)), \quad (2)$$

where θ is half the beam crossing angle, and x_c is the spatial coordinate along the crossing dimension shown in Fig. 1.

The entire electric field of the unknown pulse, consisting of both the phase and spectral amplitude can be retrieved from Eq. (2) by isolating the argument and amplitude of the cosine term. This is done by applying a one-dimensional Fourier transform along the x_c -dimension [7,9]. Once in k -space, the phase and non-phase information (the first two terms in Eq. (2)) from the interferogram separate out as illustrated in Fig. 2(b). Either of the side-bands is isolated from the rest of the data and then Fourier transformed back to the position domain. This results in the product of the unknown and reference pulse complex fields. Additionally,

using FROG, the phase of the field of the reference pulse must be measured, and divided out, thereby completely characterizing the unknown pulse.

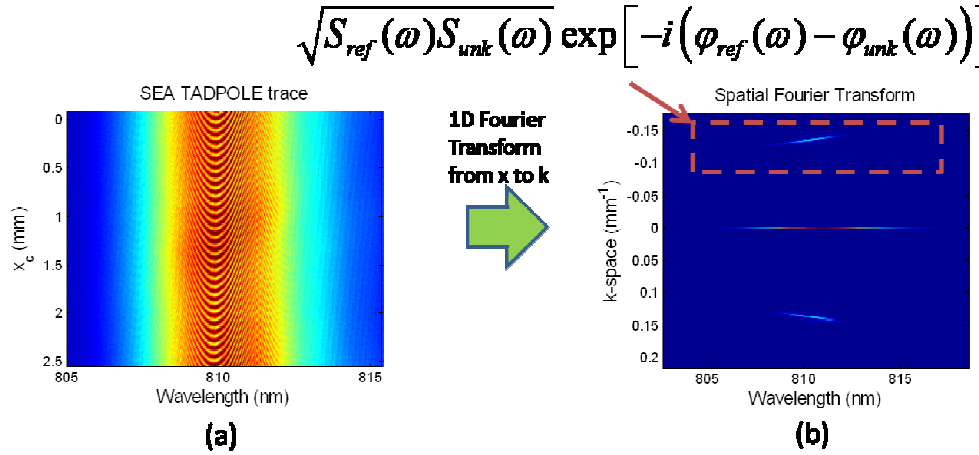


Fig. 3. Retrieving the phase and spectrum in SEA TADOLE. A typical SEA TADPOLE trace of a heavily chirped pulse is shown in 3(a). Fig 3(b) shows how the one-dimensional spatial Fourier transform separates the data into three bands. The side-bands contain both the spectral phase difference and the spectrum of the unknown pulse, and so one of these is kept, and then inverse Fourier transformed back to the position domain. Due to the fibers, no spatial information about the pulse is present, so we sum the resulting field over the camera's position axis. At this point, the known reference pulse's field is divided out in order to extract the unknown pulse's intensity and phase.

A typical MUD TADPOLE data set consists of N SEA TADPOLE traces like the one shown in Fig. 3(a). Figure 2 illustrates the multiple SEA TADPOLE traces. Since the reference pulses are successively delayed in time by a constant, τ_{ref} , each retrieved spectrum, $S_i(\omega)$, and spectral phase difference,

$$\Delta\varphi_i(\omega) = \varphi_{unk_i}(\omega) - \varphi_{ref_i}(\omega), \quad (3)$$

corresponds to a measurement of the unknown pulse at a different time, τ_i . Here τ_i is the delay between the reference and unknown pulse for the i^{th} SEA TADPOLE trace. Each SEA TADPOLE trace combined with a FROG measurement of the reference pulse determines the spectral phase of the unknown pulse, $\varphi_{unk}(\omega)$, yielding the entire electric field,

$$E_i(\omega) = \sqrt{S_i(\omega)} e^{i\varphi_i(\omega)}. \quad (4)$$

At the spectrometer, the duration of each reference pulse in time is given by τ_{sp} . Each reference pulse interferes with the unknown pulse over a temporal width of τ_{sp} . Therefore, each $E_i(\omega)$, will contain spectral information about the unknown pulse in the time window,

$$\tau_i - \frac{\tau_{sp}}{2} < t < \tau_i + \frac{\tau_{sp}}{2}. \quad (5)$$

Therefore, the first step of the MUD TADPOLE retrieval algorithm yields N measurements of the electric field of the unknown pulse centered about different times, $E_{i=1:N}(\omega)$.

3.2 Temporal filter

The second step of the MUD TADPOLE algorithm involves temporal filtering each of the N measurements described above. In this step, the retrieved electric fields are Fourier transformed from the spectral domain into the time domain. This results in electric fields

centered about each τ_i . Because the reference pulse interferes with a section of the unknown pulse of length τ_{sp} , which is smaller than the time-axis of the retrieved pulse, only information within this region is kept while that from larger and smaller times is discarded. Specifically, we crop each field so that:

$$\tilde{E}_i(t) = \begin{cases} \tilde{E}_i(t) & \text{for } \tau_i - \frac{\tau_{sp}}{2} < t < \tau_i + \frac{\tau_{sp}}{2} \\ 0 & \text{otherwise} \end{cases} . \quad (6)$$

After temporally filtering, each retrieved electric field is shifted in time because the field retrieved by the i^{th} reference pulse, $\tilde{E}_i(t)$, is centered around $t = 0$, the local zero time value of the reference pulse. In other words, the i^{th} retrieved field, $\tilde{E}_i(t)$, is measured in a time frame relative to the i^{th} reference pulse. Since the goal of MUD TADPOLE is to piece together the entire unknown pulse in time, the retrieved fields must be transformed from the local time frame of each reference pulse to the lab frame in which all of the reference pulses occur at different times. This means that the i^{th} retrieved field, $\tilde{E}_i(t)$, is linearly shifted by τ_i ,

$$\tilde{E}_i(t) \Rightarrow \tilde{E}_{i,\text{lab}}(t - \tau_i). \quad (7)$$

3.3 Concatenation

Although the spectrum and phase of the pulses from the mode-locked laser are quite stable, slight non-uniformity of the spatial fringes over a significant period of time, noise, and shot-to-shot jitter of the reference pulses cause discontinuities when concatenating the fields. To reduce these discontinuities we use a weighted averaging scheme.

Since each $\tilde{E}_{i,\text{lab}}(t - \tau_i)$ corresponds to an independent measurement by the i^{th} reference pulse from the laser, each retrieved field is weighted by a Gaussian weighting function with a half width at $1/e$, τ_G , which is less than τ_{sp} and centered on the i^{th} reference pulse

$$G_i(t - \tau_i) = \exp\left[-\left(\frac{t - \tau_i}{\tau_G}\right)^2\right]. \quad (8)$$

The weighting function was chosen to be a Gaussian function because the temporal response function is approximately Gaussian in form [12,24].

The accuracy of the experimental results are unaffected by variation of the width of the Gaussian weighting function as long as the width is less than τ_{sp} , and greater than or equal to the delay spacing between the reference pulses, τ_{ref} , or,

$$\tau_{ref} \leq \tau_G < \tau_{sp}. \quad (9)$$

Because the delay between reference pulses, τ_{ref} , is less than τ_{sp} , a given section of the unknown pulse is reliably retrieved by more than one reference pulse. Therefore, we average together this redundant information to obtain a better retrieval. But due to the spectrometer's finite resolution, the accuracy of an individual measurement decreases as you move away from its temporal origin. The purpose of the weighting function is to account for this. Therefore, we choose the weighting function to be Gaussian (rather than square) so that it more heavily weighs information that originates from the temporal center of the individual measurements. And keeping the weighting function's width less than τ_{sp} , assures that no information from delays greater than τ_{sp} , are included in the average, because this information is outside the spectrometer's temporal window and therefore, not accurate. This process reduces the noise in the retrieval and helps to avoid discontinuities when concatenating the independent measurements together.

Since τ_{sp} is directly related to the spectral resolution of a spectrometer, it can be obtained by measuring the fringe contrast of interference spectra at different delays [12,24]. In our experiment we measured $\tau_{sp} = 9.2$ ps. Therefore, using a delay spacing of $\tau_{ref} = 1.46$ ps satisfied the condition that $\tau_{ref} < \tau_{sp}$.

Finally, the retrieved fields are concatenated together. We do this by separating each $\tilde{E}_{i,lab}(t - \tau_i)$ into its constituent phase and amplitude,

$$\tilde{E}_{i,lab}(t - \tau_i) = A_i(t - \tau_i)e^{i\varphi_i(t - \tau_i)}. \quad (10)$$

Before concatenating the phase, each measured phase, $\varphi_i(t - \tau_i)$, must be re-phased (that is, its zeroth-order phase value is matched to that of the neighboring pulselet). The reason for this is that our interferometer is not actively stabilized. Therefore, there is a slow drift in the phase over the course of an entire MUD TADPOLE scan, just as there is in SEA TADPOLE [7,14].

Accordingly, the retrieved temporal phases have a different absolute phase, which must be removed before concatenation. This can be done easily because the temporal sections of the unknown pulse measured by subsequent reference pulses overlap. Therefore, the absolute phase of two individual measurements of the same time are set equal, which effectively removes the effect of drift in MUD TADPOLE.

This re-phasing procedure uses the fact that the absolute temporal phase does not contain any frequency vs. time information [5]. Therefore, before concatenating, the absolute phases, $\varphi_i^{(0)}$, where,

$$\varphi_{i+1}(t - \tau_i) = \varphi_i^{(0)} + \varphi_i^{(1)}(t - \tau_i) + \varphi_i^{(2)}(t - \tau_i)^2 + \dots, \quad (11)$$

are re-phased. Specifically, the absolute phase of the $i^{th}+1$ retrieved field, $\varphi_{i+1}^{(0)}$, is set equal to that of the previous retrieved phase at the midway point between the two, or:

$$\varphi_{i+1}^{(0)}\left(\frac{\tau_{i+1} + \tau_i}{2}\right) = \varphi_i^{(0)}\left(\frac{\tau_{i+1} + \tau_i}{2}\right). \quad (12)$$

This re-phasing is performed sequentially, beginning with φ_2 and ending with φ_N .

After re-phasing, both the phases, $\varphi_i(t - \tau_i)$, and amplitudes $A_i(t - \tau_i)$, are separately superposed using a weighted average, yielding the entire temporal amplitude of the unknown pulse:

$$A_{final}(t) = \frac{\sum_{j=1}^N G_j(t - \tau_j)A_j(t - \tau_j)}{\sum_{i=1}^N G_i(t - \tau_i)}, \quad (13)$$

$$\varphi_{final}(t) = \frac{\sum_{j=1}^N G_j(t - \tau_j)\varphi_j(t - \tau_j)}{\sum_{i=1}^N G_i(t - \tau_i)}. \quad (14)$$

The product of the amplitude and phase yields the entire temporal amplitude and phase of the unknown pulse.

$$\tilde{E}_{final}(t) = A_{final}(t)e^{i\varphi_{final}(t)}. \quad (15)$$

Figure 2 graphically represents the MUD TADPOLE retrieval algorithm.

4. Experimental setup

We performed experiments using a Coherent MIRA Ti:Sapphire oscillator. The pulses were centered at 805 nm, with a FWHM bandwidth of 6 nm. Using a Swamp Optics GRENOUILLE 8-50USB [25], the input pulse was measured to have a temporal width of 168 fs. The pulses were stretched to a FWHM length of 40 ps using a single-grating pulse compressor [26].

The SEA TADPOLE set-up shown in Fig. 1 is described in more detail in [7]. Specifically, for our set-up we used a 250 mm focal-length spherical lens to collimate and cross the beams emanating from the fibers. Additionally, a 600 grooves/mm grating and 200 mm focal-length lens were used for mapping wavelength to position in the spectrometer. The delay stage used was a Newport MFA Series Miniature Linear Stage with a Newport ESP100 single-axis controller.

5. Results and discussion

We performed two experiments to demonstrate MUD TADPOLE's unique capabilities relative to a conventional high-resolution spectrometer and to SEA TADPOLE. These experiments demonstrate how MUD TADPOLE overcomes the limitations of a conventional spectrometer as well as those of SEA TADPOLE. In both experiments MUD TADPOLE provides the necessary spectral resolution to completely characterize the intensity and phase of the unknown pulse.

In the first experiment, we measured the stretched 40 ps pulse using MUD TADPOLE with 100 SEA TADPOLE traces each having a different reference-pulse delay using the set-up shown in Fig. 1. The reference pulses were separated in time by 1.46 ps. This temporal spacing was chosen to provide a significant amount of overlap with neighboring reference pulses, thereby reducing discontinuities during the concatenation routine, which is helpful, but not necessary. The half width at 1/e of the weighting function was chosen to be equal to the temporal separation of the reference pulses, $\tau_G = 1.46$ ps.

Figure 4(a) shows the retrieved temporal amplitude and phase of the 40 ps pulse. Since there is no commercial device capable of measuring the full intensity and phase of such a pulse, we compared the retrieved spectrum to that of an Ocean Optics HR 4000 spectrometer shown in Fig. 4(b). In this instance, the spectrometer provided enough spectral resolution to accurately measure the relatively smooth spectrum of the pulse. This is because the pulse compressor modifies the spectral phase rather than the spectral intensity. The result is that the linearly chirped pulse did not have finer spectral intensity features than the resolution of the spectrometer. Instead, the spectral phase of the chirped pulse contained the fine spectral features, which the spectrometer is unable to measure. In contrast, MUD TADPOLE is able to measure the phase, as demonstrated by the complete measurement of the temporal intensity and phase of the 40 ps pulse shown in Fig. 4(a).

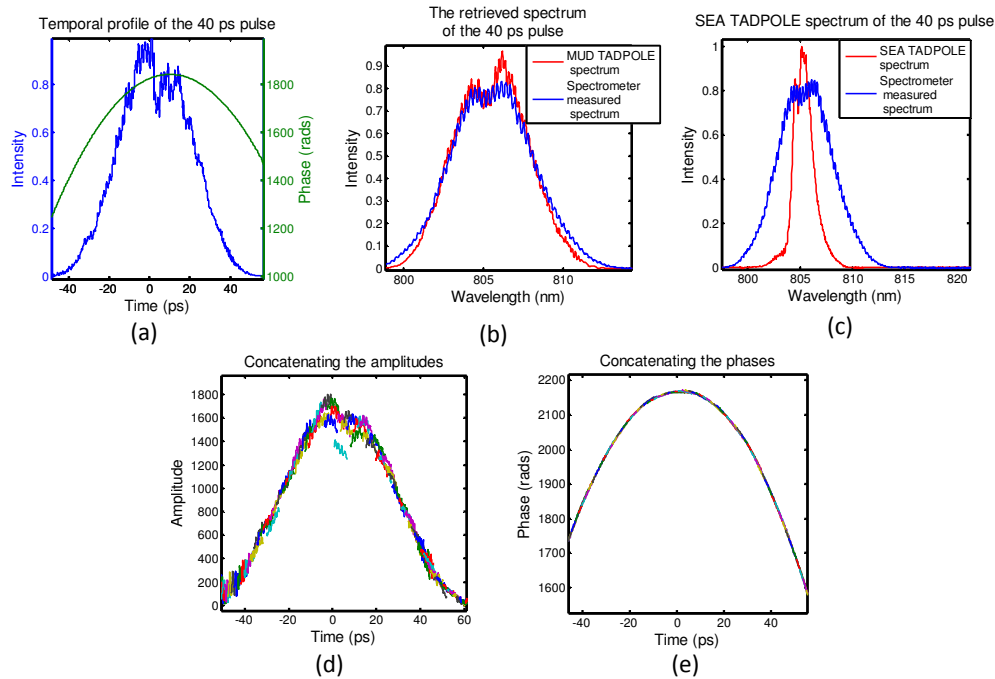


Fig. 4. a. The MUD TADPOLE-retrieved temporal amplitude and phase of a chirped 40 ps pulse. b. The MUD TADPOLE-retrieved spectrum compared to an independently measured spectrum using a spectrometer. c. The measured SEA TADPOLE spectrum compared to the independently measured spectrum. The overly narrow SEA TADPOLE spectrum shows the need for MUD TADPOLE. d. Concatenation of the retrieved temporal amplitudes, $A_i(t-\tau_i)$. Similar to Step 3 in Fig. 2, each color represents the retrieved amplitude at a different delay, which shows the multiple measurements overlapping in time as discussed in Section 3.3. e. Concatenation of the retrieved temporal phases after re-phasing, $\phi_i(t-\tau_i)$.

Figure 4(c) highlights the limitations of SEA TADPOLE compared with MUD TADPOLE. It shows the spectrum measured by SEA TADPOLE and also by a spectrometer. It is clear that the spectrum retrieved from SEA TADPOLE is too narrow. Since the 40 ps pulse was highly chirped, different colors occurred at different times in the pulse, and the reference pulse inside the spectrometer of SEA TADPOLE stretched only long enough to interfere with ~ 1.9 nm of the chirped-pulse spectrum. The other wavelengths are missing from the SEA TADPOLE spectral measurement. In contrast, Fig. 4(b) shows that MUD TADPOLE retrieves the entire 40 ps pulse.

Figure 4(d) and 4(e) show the concatenation of both the amplitude and phase used in Step 3 of the concatenation routine. As illustrated in Fig. 2, the amplitudes and phases were individually concatenated, and the different colors represent different measurements made with each individual SEA TADPOLE trace.

Our next experiment highlighted the large temporal range and high temporal resolution of MUD TADPOLE. Additionally, it also exposes the limitations of a conventional spectrometer. In this experiment we measured a chirped double pulse at multiple delays. At delays larger than 40 ps, the double pulse exhibited fine spectral-intensity features that were resolvable by MUD TADPOLE, but unresolvable by a conventional spectrometer.

The double pulse was generated by placing a Michelson interferometer after the single-grating pulse compressor. For this experiment we reduced the bandwidth of the incident pulse to 3.4 nm in order to fit the entire pulse within the temporal range of MUD TADPOLE, which is limited by the scanning range of our delay stage. As a result, we used a 300 mm focal

length cylindrical lens inside the spectrometer to further spread out the reduced bandwidth on the camera.

In contrast to the previous measurement shown in Fig. 4, the reduced bandwidth of the incident pulse on the compressor resulted in the stretching of the incident pulse to 22 ps FWHM.

Figure 5 shows both the measured and simulated temporal intensity and phase of two linearly chirped pulses at variable delays with respect to one another. Fig. 5 demonstrates a phenomena known as chirped pulse beating [27], which occurs because at each point in time the frequency content of each pulse differs by a constant beat frequency. This beat frequency is proportional to the delay, τ , between the two pulses.

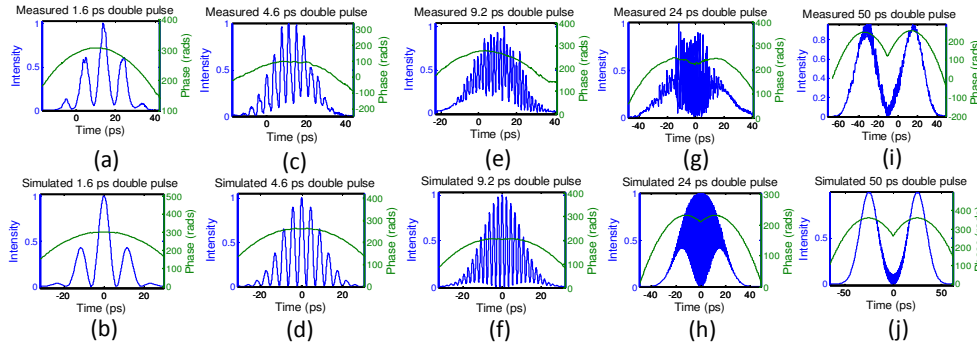


Fig. 5. A comparison of the measured and calculated temporal profiles of a chirped double pulse at variable delays. a,b. The MUD TADPOLE retrieved and simulated temporal profile of two 22 ps linearly chirped pulses separated by 1.6 ps. c,d. The retrieved and simulated temporal profile after increasing the delay between pulses to 4.6 ps. e,f. The retrieved and simulated temporal profile after increasing the delay between pulses to 9.2 ps. g,h. The retrieved and simulated temporal profile after increasing the delay between pulses to 24 ps. At this large delay the temporal phase develops a cusp which MUD TADPOLE is able to retrieve. i,j. The retrieved and simulated temporal profile of a 50 ps double pulse. At such a large delay the temporal beating is not as noticeable as at much shorter delays because fewer frequencies are temporally overlapped. In all examples the agreement between the retrieved and simulated results is good. These results simultaneously highlight the extended temporal range and high temporal resolution of MUD TADPOLE.

Figure 5 simultaneously highlights the high temporal resolution and the large temporal range of MUD TADPOLE. The temporal resolution of MUD TADPOLE is determined by the spectral range of the spectrometer used in Fig. 1. In this experiment our spectrometer had a spectral range of 30 nm and a temporal resolution of 71 fs. This high temporal resolution was put to good use in the measurement of the double pulse with a 24 ps delay shown in Fig. 5(g). The fast temporal beating which had a temporal period of 622 fs is well resolved by MUD TADPOLE.

A double pulse afforded us another opportunity to check the validity of our measurements. Using an optical power meter, the ratio of the intensities of the two pulses in the double pulse was found to be 0.99, or almost equal. MUD TADPOLE confirms this measurement as shown in Fig. 5(i), where the intensities of the retrieved fields are shown to be roughly equal.

Another interesting aspect to note is that MUD TADPOLE has the capability to measure pulses with phase cusps shown in Fig. 5(g) and 5(i).

Although the experimental and simulated results agree quite well, there is some disagreement, which is attributed to the slight instability of the Michelson interferometer used to make the double pulse. The use of an actively stabilized interferometer to make the double pulse would result in better agreement between our simulations and experimental results.

Figure 5(i) highlights the long temporal range of MUD TADPOLE, which is an equivalent measure of its spectral resolution. This fact is better explained by examining the spectrum corresponding to the 50 ps double pulse.

Figure 6(a) and 6(b) show both the retrieved temporal profile and the retrieved spectrum of the 50 ps double pulse. Since the two pulses are separated by such a large time delay, the spectral fringes are too fine for the high-resolution Ocean Optics spectrometer to resolve; the spectral fringes due to a double pulse measured by a spectrometer with .01 nm spectral resolution wash out completely at around 40 ps. In contrast, MUD TADPOLE resolves them accurately.

Apart from the spectral fringes, Fig. 6(b) shows that the envelope of the MUD TADPOLE-retrieved spectrum and that of the spectrometer measured spectrum agree, as they should.

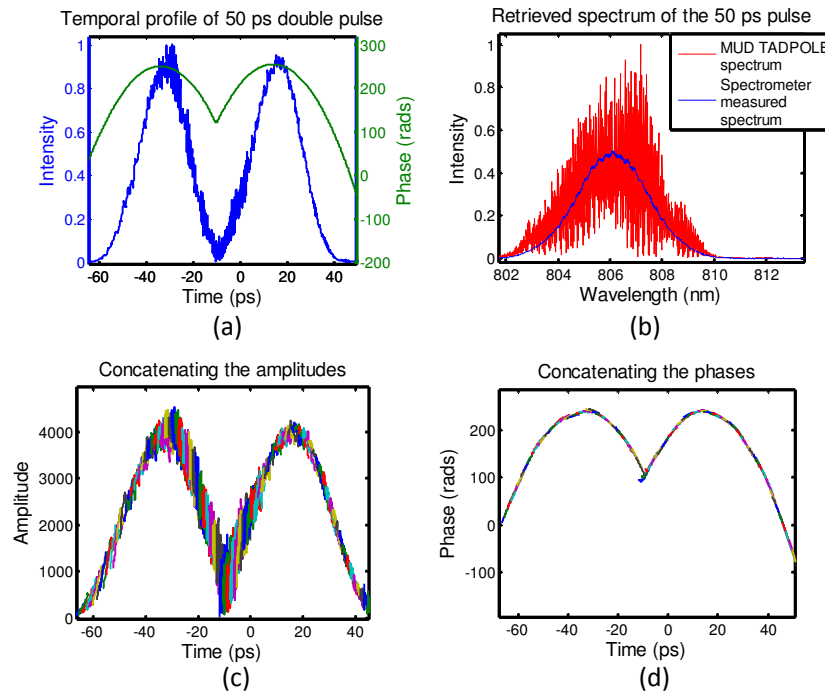


Fig. 6. a. The MUD TADPOLE-retrieved temporal intensity and phase of a 50 ps chirped double pulse. b. The retrieved spectrum compared to an independently measured spectrum. The spectrum shows the high spectral resolution of MUD TADPOLE, and it highlights a conventional spectrometer's limitations. c. Concatenation of the retrieved temporal amplitudes, $A_i(t-\tau_i)$. Similar to Step 3 in Fig. 2, each color represents the retrieved amplitude at a different delay. e. Concatenation of the retrieved temporal phases after re-phasing, $\phi_i(t-\tau_i)$.

Additionally, the measurement of the temporal phase of each of the pulses (shown in green in Fig. 6(a)) gives us more confidence in MUD TADPOLE. We expect the measured temporal chirp to be almost equal, given that both pulses were chirped equally by the single grating pulse compressor. Although the chirp of the two pulses is not exactly the same due to the geometry of a Michelson interferometer, where one pulse makes three passes through a partially reflecting 1 cm beam splitter, while the other pulse makes only a single pass, this amount of added chirp is negligible compared to that introduced by the pulse compressor.

Figure 6(c) and 6(d) show the concatenation of both the amplitude and phase used in Step 3 of the concatenation routine. As illustrated in Fig. 2, the amplitudes and phases were

individually concatenated. Fig. 6(d) shows that the concatenation routine described in section 3.3 is able retrieve phases with cusps.

6. Summary, limitations, and future work

In summary we have used a variation of SEA TADPOLE that we call MUD TADPOLE to completely characterize pulses up to 100 ps in length with 71 fs resolution, achieving a length-to-resolution ratio of over 1400. MUD TADPOLE has successfully measured complex pulses with time-bandwidth products of ~ 700 .

There is no fundamental limit to the length (or complexity) of a pulse that can be measured by MUD TADPOLE. Experimentally, the limit is given by the scanning range of the delay stage in Fig. 1. This limit will also depend on the dynamic range of the camera, because for extremely long pulses, the fringes will not be visible in the presence of potentially more intense DC terms. As the unknown pulse duration increases, the fringe contrast for each measurement will decrease, because fringes only occur at times where the pulses temporally overlap (τ_{sp}), so most of the intensity will be in the DC. In the perfect case where the reference pulse temporally overlaps with the entire unknown pulse, the ratio between the signal term and the DC term will be 1/2. But if the unknown pulse duration is $1000\tau_{sp}$, the ratio between the DC and signal term will be 1/2000 requiring a dynamic range of more than 2000 (greater than 10 bits). In other words, a 10 bit camera (maximum of 1024 counts) could measure a pulse of maximum length $500\tau_{sp}$. For this latter case, for a pulse with a bandwidth of 5nm, and $\tau_{sp} = 10$ ps, the maximum TBP of a pulse that can be measured using MUD TADPOLE is $\sim 70,000$.

Additionally, there is no fundamental limitation to the spectral range, or equivalently, the temporal resolution of the device. Experimentally, the spectral range is limited by the camera size. By choosing a camera with a larger array size, MUD TADPOLE could accommodate larger bandwidths.

One fundamental limitation of MUD TADPOLE is that it is an interferometric method that requires a well-characterized reference pulse. Therefore, it can only measure pulses that are temporally and spectrally overlapped with the reference pulses. Furthermore, since MUD TADPOLE is a multi-shot method, it requires the unknown source to be stable over the entire scanning range of the delay stage. The experiments performed in this paper lasted about 15 minutes and consisted of 100 traces. This makes it ideal for measuring pulses modified by a time-stationary filter [28], such as a pulse stretcher and/or compressor [26]. In contrast, pulses generated from phenomena with rapid variations from shot to shot, like continuum generation [29], may be difficult to measure accurately using MUD TADPOLE.

Additionally, an experimental limitation of MUD TADPOLE is imposed by the accuracy of the delay stage. The accuracy of the delay stage is important with regards to Step 2 of the MUD TADPOLE retrieval algorithm described in Section 3.2. In this step, each retrieved temporal electric field is temporally shifted from the reference pulse time frame to the lab frame. It is important that the accuracy of the time delay control (the delay stage in Fig. 1) be much less than the temporal resolution of MUD TADPOLE. Otherwise, each retrieved field will not be properly shifted resulting in discontinuities when concatenating.

The scanning stage used had an accuracy of $0.035\mu\text{m}$ corresponding to a delay accuracy of 0.12 fs. This is sufficient as it is much less than the temporal resolution of MUD TADPOLE which was 71 fs considering the spectral range of the spectrometer was 30 nm.

A modified version of the MUD TADPOLE retrieval algorithm could be applied to dual quadrature spectral interferometry [13] to increase its temporal range or equivalently its spectral resolution. The only modification in the setup would be an additional delay stage in the reference arm of the Mach-Zehnder interferometer to provide the variable delay.

In contrast, Fourier-transform spectral interferometry (FTSI) [6] could *not* be improved in this manner because a large delay is required between the reference and unknown pulses, and this cannot be scanned, because the Fourier retrieval algorithm requires filtering along the

spectral dimension. In contrast, MUD TADPOLE does not have this limitation, because its filtering is performed in the spatial domain.

In the future, we plan to implement MUD TADPOLE in a manner similar to [14] in order to measure the full spatio-temporal field of long complex pulses and also to modify it for single-shot measurements.

We believe that this simple, compact, and inexpensive device can measure pulses with time-bandwidth products in excess of 70,000 using inexpensive, off-the-shelf components. Also, it could improve the spectral resolution of any spectrometer by a large factor.